

Study of the Heat Transfer of a Two-Tubular Exchanger with a Hemispherical End Buried

Dhahri Imen

Applied Mechanics and Engineering Laboratory, National Engineering School of Tunis, University of Tunis-El Manar, Tunis, Tunisia

Email: imendh@gmail.com

How to cite this paper: Imen, D. (2022) Study of the Heat Transfer of a Two-Tubular Exchanger with a Hemispherical End Buried. *Energy and Power Engineering*, 14, 705-718.

<https://doi.org/10.4236/epe.2022.1411038>

Received: October 14, 2022

Accepted: November 26, 2022

Published: November 29, 2022

Copyright © 2022 by author(s) and Scientific Research Publishing Inc.

This work is licensed under the Creative Commons Attribution International License (CC BY 4.0).

<http://creativecommons.org/licenses/by/4.0/>



Open Access

Abstract

In this paper, a numerical study of a buried hemispherical double-pipe heat exchanger with soil by using geothermal energy is presented. Since the local air-wall exchange coefficient throughout the heat exchanger is unknown, a study of mathematics based on the theory of Green's functions in the unsteady state was developed. The complexity of the geometry has led us to develop a numerical study that allows us to obtain results that reflect the importance of heat exchange. The applications are numerous, especially in the storage of energy in the soil to optimize greenhouses according to the cycle of the seasons.

Keywords

Laminar Forced Convection, Nusselt Number, Horizontal Heat Exchanger, Temperature Distribution

1. Introduction

Coaxial tubes have design advantages over U-tube design for shell-and-tube heat exchangers because there is only one inlet instead of two for each tube. In this study, the various heat transfer mechanisms and flow conditions are described to determine the temperature distribution of a spherical-head tubular heat exchanger for various thermal parameters, considering heat exchange.

The problem of forced convection in horizontal tubes or horizontal cylindrical ring geometries has received much attention in recent years due to its importance in many industrial applications, especially in power generation (nuclear power plants, etc.) and air conditioning (buildings, greenhouses, etc.).

This paper is concerned with the study of forced convection air flow in a buried double-pipe exchanger. Wall temperature and wall heat flux are unknown

and change with time. In addition, the heat transfer coefficient (fluid-wall) is also unknown. In this context, the solution of the problem of heat transfer of a laminar flow in a buried coaxial exchanger, where both wall temperature and wall heat flux are unknown, is based on the study of Mnassri [1], which was validated by an experimental study of Desmos [2], which allowed us to propose a correct correlation for the transfer coefficient $h(z, t)$.

Shankar [3] studied the heat transfer of a fluid in laminar flow through a cylindrical tube. A simple version of this problem was analyzed by Graetz and validated in this work to define the heat transfer coefficient as a function of the Péclet number.

The study of Sieder and Tale [4] and the model of Von Hausen [5] are corrected by Ginelsky [6] to give a complete formulation of the Nusselt number in the laminar regime as a function of Gz (Graetz criterion) for various conditions at the boundaries with the wall.

Kim [7] determined the Nusselt number for the thermal and hydrodynamic evolution of a fluid by solving the Graetz-Nusselt problem in a cylindrical shell containing a bundle of seven parallel tubes with constant heat flow boundary conditions at the surface.

His results were compared with those obtained by the finite difference method.

In this study, the complexity of the geometry of the system and the infinity of the environment of the heat exchanger led us to combine the finite volume method with the finite element method based on the theory of Green's functions to solve the problem.

Numerical calculations were performed using the code CFD to determine the temperature distribution as a function of various parameters such as the heat transfer coefficient, Reynolds number, inlet temperature, and thermal conditions on the wall such as temperature to verify the reliability, accuracy and physical reality of the proposed idea.

2. Description of the Exchanger

Our system is a bitube exchanger consisting of two concentric tubes with hemispherical ends embedded in the ground (**Figure 1**). The inner tube is considered thermally insulating, has a diameter of 40 mm and a length of 1960 mm, and is located inside a steel tube with a diameter of 80 mm and a length of 2000 mm and a thickness of 3 mm.

The hot fluid enters the inner tube at a temperature $T_c(t)$, circulates from right to left, returns to the annulus from left to right at an average velocity U_0 , and exits at an exit temperature $T_e(t)$. The storage medium (soil) forms a domain (D) bounded by an interface (S).

3. Mathematical Formulation of the Problem

This part of the work is based on a study carried out by Mnassri [1].

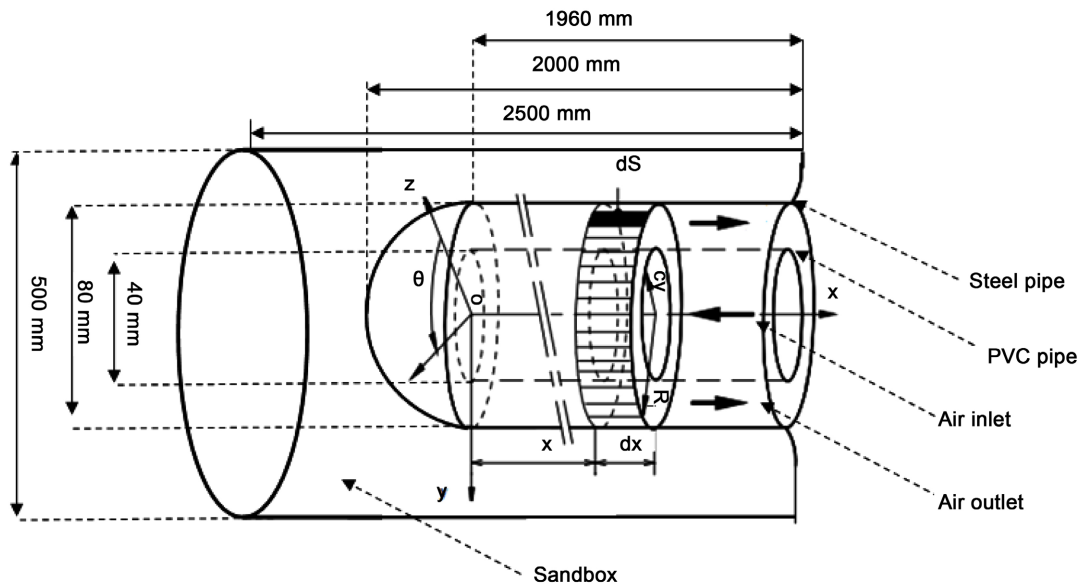


Figure 1. Geometry of the exchanger.

The ground is supposed homogeneous and isotropic solid medium and its thermal characteristics are considered stable and independent of the temperature. This medium of storage constitutes a domain (D) surrounded by a boundary surface (S) (Figure 1). The surface (S) is the union of the free surface of the soil (St) and the surface of the buried exchanger (Se);

$$(S) = (Se) \cup (St).$$

3.1. Energy Propagation Equation in the Stock

The equation of heat propagation in it is:

$$\frac{1}{a_{s,0}} \frac{\partial T(\vec{r}, t)}{\partial T} - \Delta T(\vec{r}, t) = 0 \tag{1}$$

The Green function $G(\vec{r}, \vec{r}', t)$, the solution of the associated Equation (2):

$$\frac{1}{a_{so}} \frac{\partial G(\vec{r}, \vec{r}', t)}{\partial T} - \Delta G(\vec{r}, \vec{r}', t) = \delta(\vec{r} - \vec{r}') \tag{2}$$

$G(\vec{r}, \vec{r}', t)$ represents, physically, the response of the medium to a heat impulse on the point \vec{r}' at the instant $t = 0$. One supposes it is defined in the domain (D), containing the points \vec{r} and \vec{r}' , limited by surface (S). $G(\vec{r}, \vec{r}', t)$ is such that it is null for $t < 0$ and tends towards $\delta(\vec{r} - \vec{r}')$ at $t = 0$. If we apply the Laplace transform to the Equations (1) and (2) and we combine them and then we integrate on \vec{r} in the domain (D) limited by surface (S) we obtain:

$$\begin{aligned} \bar{T}(\vec{r}', p) = & \iiint_{(D)} \bar{G}(\vec{r}, \vec{r}', p) \frac{T_0(\vec{r})}{a_{so}} d^3r \\ & + \iint_{(S_t)} [\bar{G}(\vec{r}, \vec{r}', p) \bar{\nabla} T(\vec{r}, p) - T(\vec{r}, p) \bar{\nabla} \bar{G}(\vec{r}, \vec{r}', p)] \bar{n} ds \\ & + \iint_{(S_e)} [\bar{G}(\vec{r}, \vec{r}', p) \bar{\nabla} T(\vec{r}, p) - T(\vec{r}, p) \bar{\nabla} \bar{G}(\vec{r}, \vec{r}', p)] \bar{n} ds \end{aligned} \tag{3}$$

We obtain the expression for the temperature of the heat exchanger surface (tube wall):

$$T_u(\vec{r}', t) = 2F(\vec{r}', t) + 2 \int_0^t \iint_{(Se)} \left[G(\vec{r}, \vec{r}', t - \tau) \vec{\nabla} T(\vec{r}, \tau) - T(\vec{r}, \tau) \vec{\nabla} G(\vec{r}, \vec{r}', t - \tau) \right] \vec{n} ds d\tau \quad (4)$$

where:

$$F(\vec{r}', t) = \iiint_{(D)} G(\vec{r}, \vec{r}', t) \frac{T_0(\vec{r})}{a_{so}} d^3r - \int_0^t \iint_{(St)} T(\vec{r}, \tau) \vec{\nabla} G(\vec{r}, \vec{r}', t - \tau) \vec{n} ds d\tau \quad (5)$$

3.2. Boundary Conditions at the Free Surface and at the Exchanger Surface

We consider on (St) the case where the surface temperature is imposed and equal to $T_a(\vec{r}, t)$: This boundary condition imposes to $G(\vec{r}, \vec{r}', t)$ to be null on the level of the ground surface (St) . We evoke the particular case where the temperature imposed on (St) is equal to the reference temperature T_0 supposed as uniform. Consequently, $F(\vec{r}', t)$ is null.

$$T_u(\vec{r}, t) = T_f(\vec{r}, t)_{paroi} \quad (6)$$

The quantity of heat yielded by the calorific fluid is completely received by the ground. The density of heatflux, at the wall of the exchanger, is then continuous.

$$\begin{aligned} & -k_f \left[\frac{\partial T_f(\vec{r}, t)}{\partial n} \right]_{paroi} \\ & = -k_s \left[\frac{\partial T(\vec{r}, t)}{\partial n} \right]_{paroi} \end{aligned} \quad (7)$$

If we replace the intervening terms in the Relations (6) and (7) in the expression of the temperature at the wall of the Relation (4), we obtain:

$$T_u(\vec{r}', t) = 2 \int_0^t \iint_{(Se)} \left[\frac{k_f}{k_s} G(\vec{r}, \vec{r}', t - \tau) \vec{\nabla} T_f(\vec{r}, \tau) \vec{\nabla} G(\vec{r}, \vec{r}', t - \tau) \right] \vec{n} ds d\tau \quad (8)$$

3.3. Equations Governing the Fluid Flow

The fluid density ρ_f is supposed constant. The axial symmetry of the system imposes that the flow is plane ($v = 0$) and two-dimensional (r, x) . The equations governing the fluid flow can be written as follows:

$$\begin{cases} \frac{\partial u}{\partial x} + \frac{u}{r} + \frac{\partial w}{\partial r} = 0 \\ \frac{\partial P}{\partial x} = 0 \\ u \frac{\partial w}{\partial x} + w \frac{\partial w}{\partial r} = -\frac{1}{\rho_f} \frac{\partial P}{\partial r} + (g_f + g_{rf}) \left[\frac{\partial^2 w}{\partial r^2} + \frac{1}{r} \frac{\partial w}{\partial r} \right] \\ \frac{\partial T_f}{\partial t} + u \frac{\partial T_f}{\partial r} + w \frac{\partial T_f}{\partial x} = (a_f + a_{rf}) \left[\frac{\partial^2 T_f}{\partial r^2} + \frac{1}{r} \frac{\partial T_f}{\partial r} \right] \end{cases} \quad (9)$$

3.4. Boundary Conditions and Initial Conditions for the Whole System

No simplifying condition is imposed on the velocity or the temperature on the base level (annular space inlet). These boundary conditions are general and close to the practical. Uniform velocity and temperature are imposed at the inlet of the interior tube. Evidently, the regime is supposed established at the exit of the annular space because of the importance of the length of buried exchangers. Thus, the boundary conditions will be for the velocity field.

$$\begin{cases} u(r, x, 0) = w(r, x, 0) = 0 \\ u(R_i, x, t) = u(r_{ex}, x, t) = 0 \\ w(R_i, x, t) = w(r_{ex}, x, t) = 0 \\ u(r, 0, t) = U_0 \\ w(r, 0, t) = 0 \end{cases} \quad (10)$$

For the temperature field:

$$\begin{cases} T(r, x, 0) = T_0 \\ T(r, 0, t) = T_e \\ \left(\frac{\partial T}{\partial r} \right)_{r=r_{ex}} = 0 \\ T(R_i, x, t) = T_r(R_i, x, t) = 2 \int_0^t \iint_{(S_e)} \left[\frac{k_f}{k_s} G(t-\tau) \bar{\nabla} T(\tau) \bar{\nabla} G(t-\tau) \right] \bar{n} ds d\tau \end{cases} \quad (11)$$

3.5. Calculus of the Heat Transfer Coefficient

If we consider a cross section of the exchanger (**Figure 1**), the mean temperature $T_m(r, x, t)$ is the mean of various local temperatures $T(r, x, t)$ on this section.

$$T_m(x, t) = \frac{2}{U_0 (R_i^2 - r_{ex}^2)} \int_{r_{ex}}^{R_i} T(r, x, t) U(r, x) r dr \quad (12)$$

The expression for $h(x, t)$ is obtained from the expression of the heat flux density:

$$\bar{\Phi} = -k_f \bar{\nabla} T_f = -k_f \left(\frac{\partial T_f(\bar{r}, t)}{\partial r} \right)_{Paroi} \quad \bar{n} = h(T_f - T_u)_{Paroi} \quad \bar{n} \quad (13)$$

From Equations (12) and (13), the equation $h(x, t)$ (14) is determined as follows:

$$h(x, t) = \frac{\left(k_f \frac{\partial T(r, x, t)}{\partial r} \right)_{r=R_i}}{T_r - T_m} \quad (14)$$

3.6. Numerical Resolution

We benefited from the decoupling between the dynamical problem and the thermal problem: the dynamical equations were solved in the first step. However, the discretized energy equations in the fluid zone and on the exchanger sur-

face were solved in a second step.

The equations governing the velocity field were solved using the finite volume method by applying the staggered grid technique. We use a non-uniform and close-meshed grid near the inner and outer walls to account for the significant variations in velocity and temperature in the boundary layer region.

The grid used is of (30×120) . The coupling of pressure and velocity is based on the algorithm Semi-Implicit Method for Pressure Linked Revised (S. I. M. P. L. E. R).

The equations are integrated in the control volume and in the time interval $[t, t + d]$. We use an implicit diagram for the time discretization, which has the advantage of being unconditionally stable. The convective terms are discretized using an updraft diagram to ensure the stability of the numerical model.

For the discretization of the energy equation on the exchanger surface, the finite element method is used at the boundary. It consists in decomposing the exchanger surface into finite annular elements of height D . The base alone is considered as one element. Knowing the solution $T(pd)$ at a time pd , we determine the solution $T((p + 1)d)$ at the time $(p + 1)d$. Thus, stepwise from $p = 0$ to $p = n$, ($t = nd$) we obtain the solution. The discretization scheme used is an extension of the scheme used by Desmons [2]. The stability of this scheme has been studied by the same author. The iterative method used for the resolution is the line-by-line Gauss-Seidel method along the radial axis.

3.7. Results

The coefficient h is independent of T_e (for a weak temperature variation where ρ_f remains constant; which is confirmed by the correlations based on experimental data presented in the literature. In the same way, we verified numerically that this transfer coefficient is independent of the heating duration. It is constant and maintains the same value during the transient regime.

We determined, numerically, the axial evolution of the transfer local coefficient $h(x, Re)$ for $R_i/r_{ex} = 2$, $L/D_H = 50$ and various values of the Reynolds number corresponding to laminar regime ($100 \leq Re \leq 2500$) (Figure 2). We notice that:

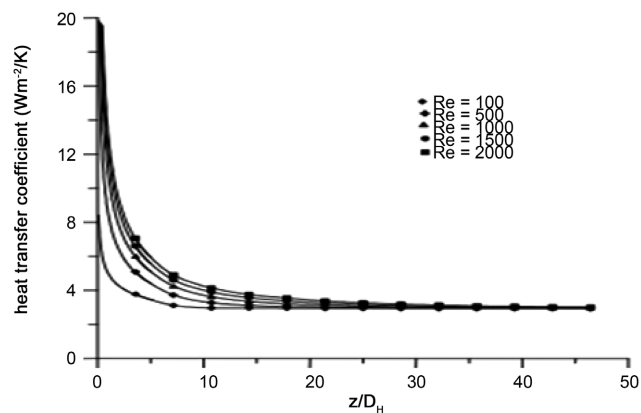


Figure 2. Variation of the heat-transfer coefficient for various Reynolds numbers. Mnassri [8].

For all Re , the curve $h(x, Re)$ tends asymptotically towards the value $2.95 \text{ W/m}^2\text{K}$ (**Figure 2**), which is close to the value $2.86 \text{ W/m}^2\text{K}$ (corresponding to the Nusselt number 4.36 often quoted in most textbooks). This value is obtained for a conductivity $k_f \gg 0.0262 \text{ W/mK}$ suitable with the air at the temperature near 27°C ($0.5 \leq (T_m - T_0)/T_0 \leq 2.5$), T_0 being equal to the ambient temperature $T_a = 19^\circ\text{C}$. The value $2.86 \text{ W/m}^2\text{K}$ corresponds to an established flow at constant flow at the wall.

4. Thermal Analysis

4.1. Analytical Study

This method of analytical calculation was developed in particular by Naili [9] who developed an analytical approach that evaluated the effect of operating parameters on the thermal power of an underground and forced convection heat exchanger, the results showed good agreement between the analytical model results and the experimental results. On the basis of this calculation method, Boughanmi [10] found an acceptable concordance of about 6% between the values of the measured and the analytically calculated heat exchanger output temperatures.

On the other hand, this analytical method was developed by Padet [11] regardless of the geometry of the exchanger, the mode of heat transfer, the flow and boundary conditions such as temperature and flow to the wall.

It is now necessary to make a number of assumptions in order to establish a simple analytical study that describes the physics of this problem, so the following assumptions are adopted:

- The heat flow is in steady state.
- The fluid is Newtonian and incompressible.
- The flow generated in the channel is laminar.
- The physical properties of the fluid are constant.

The local heat flux is exchanged through dS the small exchange surface and dx the length element of the cylinder. Is given by the following equation:

$$\begin{cases} d\Phi = U(T_0 - T_s)dS \\ d\Phi = \rho C_p V dT_{out} = \rho C_p V (T_{out}(x+dx) - T_{out}(x)) \end{cases} \quad (15)$$

suppose that there is no phase change

$$d\Phi = \rho C_p V dT_s \quad (16)$$

Both Equations (15) and (16) give:

$$d\Phi = U(T_0 - T_s)dS = \rho C_p V dT_s \quad (17)$$

$$\frac{dT_s}{T_0 - T_s} = \frac{2U}{\rho C_p V} dS \quad (18)$$

$$-\frac{dT_s}{T_s - T_0} = \frac{2U}{\rho C_p V} dS \quad (19)$$

The Equation (19) is integrated from T_e to T_s for the air, we obtain:

$$\int_{T_e}^{T_s} \frac{dT_s}{T_s - T_0} = -\frac{2U}{\rho C_p V} \int_0^x dS \quad (20)$$

$$\ln [T_s - T_0]_{T_e}^{T_s} = -\frac{2U}{\rho C_p V} dS \quad (21)$$

$$\ln \frac{T_s - T_0}{T_e - T_0} = -\frac{2U}{\rho C_p V} dS \quad (22)$$

$$\frac{T_s - T_0}{T_e - T_0} = e^{-\frac{2U}{\rho C_p V} dS} \quad (23)$$

Hence the output exit temperature of the heat exchanger will be:

$$T_s = (T_e - T_0) e^{-\frac{2h}{\rho C_p V} S} + T_0 \quad (24)$$

h is the convective heat transfer coefficient given by:

$$h = \frac{\lambda}{D_H} N_u \quad (25)$$

4.2. The Heat Transfer Coefficient

The main correlations in forced convection inside cylindrical ducts in laminar flow regime gave the temperature profiles theoretically for different boundary conditions. The classical hypothesis postulated at the wall is:

- Constant wall temperature;
- Constant heat flow.

For these two hypotheses, the theoretical studies, due to the origin of Graetz, show that, for very long tubes, the Nusselt criterion tends towards a constant value taking into account the following adimensional numbers:

$D_H = 2(R_i - r_{ex})$: the hydraulic diameter of the exchanger.

$R_e = U_0 D_H \rho / \mu$, or U_0 is the average speed in the annular pipe:

$$U_0 = \frac{(r_{ex})^2}{(R_i)^2 - (r_{ex})^2} V_e$$

- ✓ $N_u = 3.66$ for a cylindrical pipe at a constant temperature at the wall;
- ✓ $N_u = 4.36$ for a cylindrical pipe with a constant flow at the wall.

In practice, it is assumed that these values are reached when the regime is established.

With G_z denotes the Graetz critere:

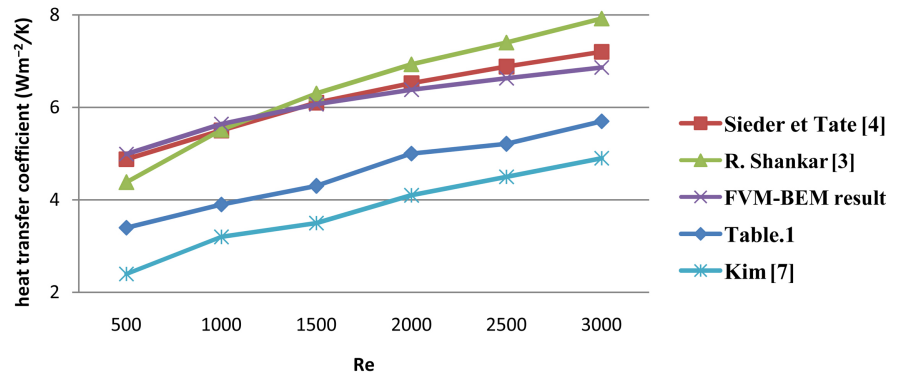
$$G_z = R_e P_r D_H / L$$

The average absolute error is 0.02 K. The results are therefore very close.

The values developed in **Table 1** in Section 4-2, of the transfer coefficient as a function of Reynolds numbers are shown in **Figure 3**. The correlations developed by Kim [7], Shankar [3], and Sieder, Tale [4] and the FVM-BEM result develop in part 1 are represented in the same figure. There is good agreement

Table 1. Expression of the nusselt number as a function of the Graetz number.

	$L/D_H > 0.03 Re$		$L/D_H < 0.03 Re$	
	$G_z < 10$	$G_z > 10$	$G_z < 100$	$G_z > 100$
Nu	3.66	$1.6 (G_z)^{1/3}$	$3.66 + \frac{0.0668 * G_z}{1 + 0.04 * (G_z)^2}$	$1.6 * (G_z)^{1/3}$

**Figure 3.** Variation of the heat-transfer coefficient versus Reynolds number.

between the various results.

5. Numerical Resolution

In this article, we are interested in numerical simulation of stationary flow and of the laminar heat transfer of a three dimensional coaxial heat exchanger with spherical end.

We chose the CFX code, available from ANSYS. This industrial software is one of the most advanced. It was selected because it offers the most opportunities for adaptation and transparency for our problem, Dhahri. I [12].

In ANSYS CFX, the simulation process is divided into four steps:

- 1) Creation of geometry and mesh.
- 2) Define the physics of the problem.
- 3) Solve the CFD problem.
- 4) Analysis and visualization of results.

5.1. Methodology of Simulation

Boundary conditions:

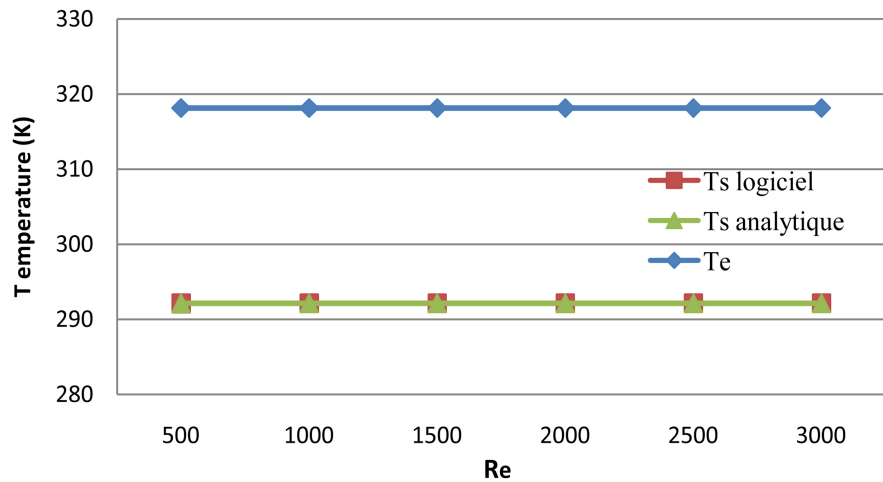
The different applied boundary conditions for this simulation are given in the following table (Table 2).

5.2. Validation of the Model

The numerical solution consists in fixing the temperature at the inlet of the heat exchanger, varying the velocity, which is a function of the Reynolds number, and then following the evolution of the temperature at the outlet of the heat exchanger. According to Figure 4, the analytical variation follows the same trend

Table 2. Details of the boundary conditions.

The inlet conditions	As part of this study, we therefore imposed the velocity in the inlet that is a function of the Reynolds number and temperature.
The outlet conditions	Here the dynamic pressure is null, which means that the total pressure is equivalent to the atmospheric pressure.
The walls conditions	Defaults these are conditions obtained via an exchange of the boundary conditions at the interface between the two solid-fluid domains of the annular space, between the fluid domain and the domain solid of the external tube which is in the one side a coefficient of heat exchange, and in the other side, a constant temperature imposed to the wall. Adiabatic conditions are placed on the interface between the two solid-fluid domains, between the fluid domain and the solid domain of the inner tube.

**Figure 4.** Variation of the inlet temperature and the outlet temperature for various of the Reynolds number.

as the numerically solved one with an acceptable agreement of the order of 0.02%.

The inlet temperature of the heat exchanger (T_e) reaches a maximum value of 323 K. While the outlet temperature of the heat exchanger (T_s) reaches a value of 293 K, there is a gain in the form of a temperature difference of the order of 35 K, reflecting the importance of heat exchange. The validation of the analytical model is limited to the energy efficiency of the heat exchanger with the cylindrical shape and the spherical end with a length of 2 m at a temperature imposed on the wall.

6. Results and Discussions

We simulated the flow and heat transfer using the module ANSYS CFX and evaluated our model in the previous section.

Then we applied our model by swapping some of the input variables such as temperature and velocity to determine the temperature distribution along our heat exchanger.

The numerical solution is to fix the temperature at the inlet of the heat exchanger, vary the velocity, which is a function of the Reynolds number, and then follow the evolution of the temperature at the outlet of the heat exchanger.

The results of **Figure 5** and **Figure 6** show the temperature distribution as a function of (x/D_H) in **Figure 5** for a Reynolds number of 3000 and for an inlet temperature of 318 K. and (**Figure 6**) for an inlet temperature of 313 K and for a change in Reynolds number between 500 and 2500.

The first part of the curves shows that the average temperature at the central tube remains practically constant and is equal to the inlet temperature. We can clearly see the effects of the lack of heat transfer (insulating wall) and the thermal resistance of the central tube. The second part of the curves shows in

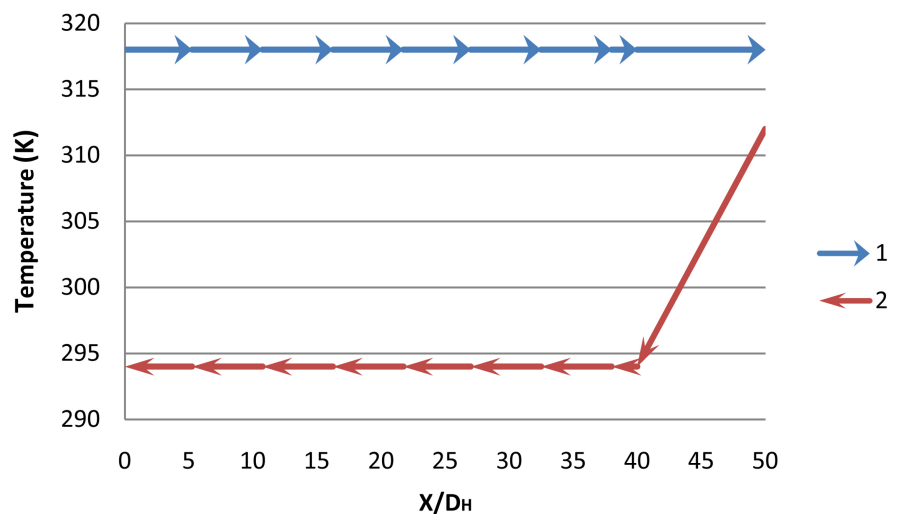


Figure 5. Local temperature variation for various of x/D_H for $T_e = 318$ K and $Re = 3000$.

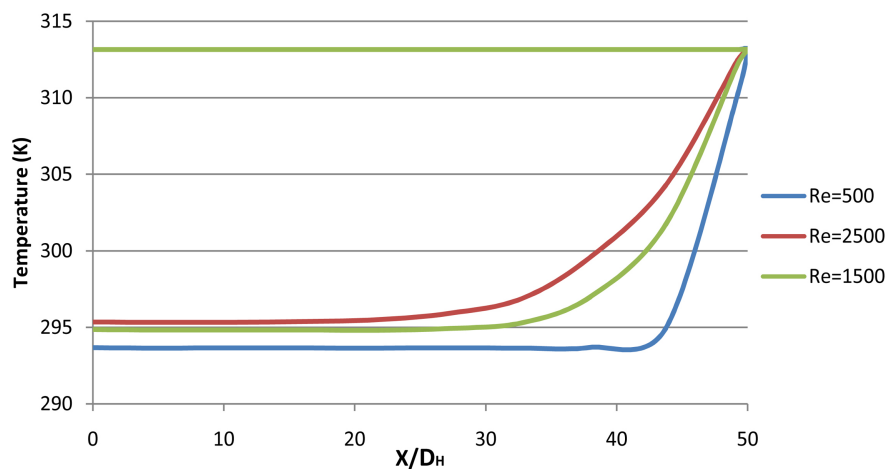


Figure 6. Temperature variation for various of x/D_H , for $T_e = 313$ K and $Re = 500$, $Re = 1500$, $Re = 2500$.

Figure 6 a variation of the Reynolds number between 500 and 2500 and for curve 2 in **Figure 5**, these results show the temperature distribution in the annulus or there is a significant decrease in the temperature that gradually moves away from the liquid recirculation zone (hemispherical end of the heat exchanger) to tend to a value close to the temperature of the wall, the temperature change is a function of both the coefficient h convective exchange and the temperature imposed on the wall.

A significant difference is observed between the temperature at the input and at the output.

The shape of the curves in **Figure 5** and **Figure 6** is similar to the temperature distribution of a countercurrent exchanger, except that the difference is at the level of the fluid recirculation zone.

Figure 7 shows a complex flow structure in which the fluid is returned from the inner tube to the outer tube via the spherical surface of the heat exchanger. This flow structure has a significant effect on the distribution of the temperature field, which decreases significantly and approaches the temperature of the wall very closely.

7. Conclusions

In this paper, we presented a study on the performance of a coaxial tube heat exchanger with spherical end with 2 m length and 40×10^{-3} m outer diameter of the central tube and 80×10^{-3} m outer diameter of the outer tube. Two approaches were used in this study:

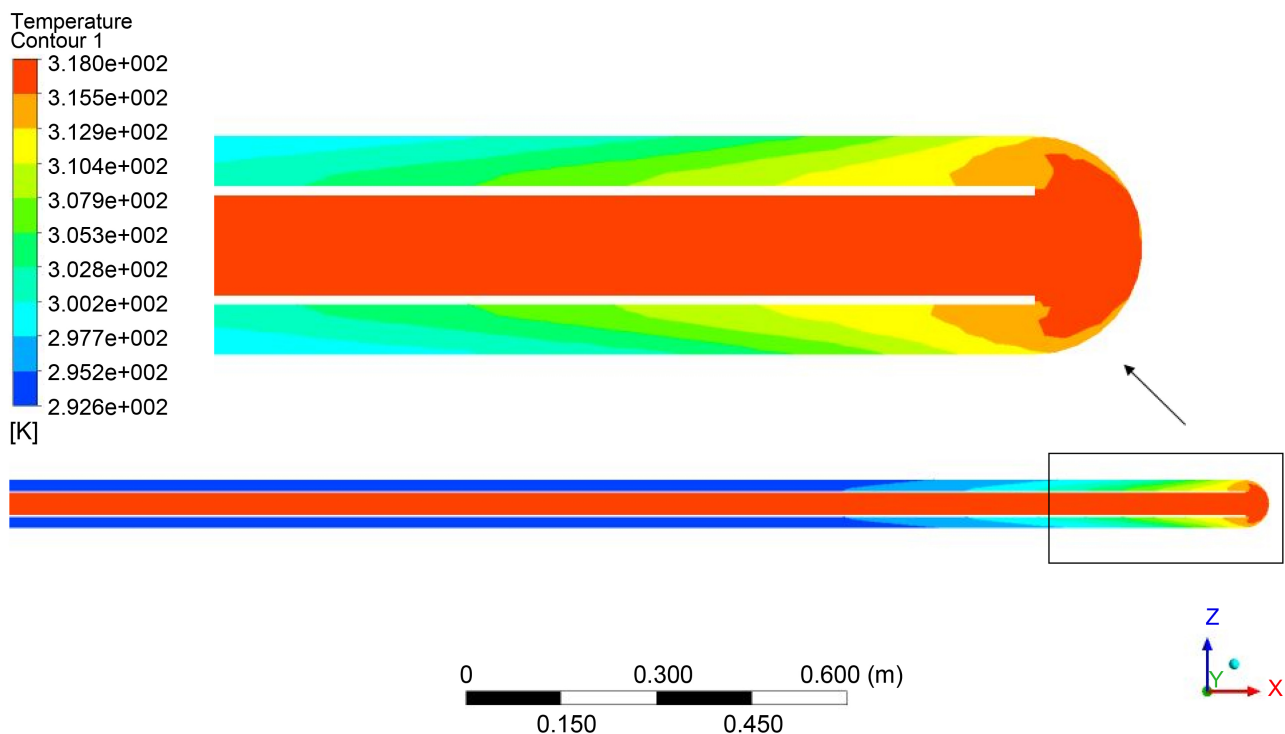


Figure 7. Distribution of the total temperature field in the exchanger for $Re = 2000$.

1) A mathematical approach by which we can calculate the heat transfer coefficient.

2) An analytical approach that allows us to calculate the outlet temperature of the heat exchanger.

3) A numerical approach based on a numerical simulation using the CFX module of the ANSYS code, which gives us the temperature distribution as a function of different parameters such as the heat transfer coefficient, the Reynolds number, the inlet temperature, the geometry and the imposed thermal conditions such as the temperature. The results show that:

- The temperature distribution at the central tube remains practically constant and corresponds to the inlet temperature.
- The temperature distribution in the annular space decreases significantly as it gradually moves away from the liquid circulation zone (spherical end of the heat exchanger) and tends to a value close to the temperature imposed on the wall.
- The analytical variation follows the same trend as the numerically solved one with an acceptable agreement of the order of 0.02%.

Conflicts of Interest

The author declares no conflicts of interest regarding the publication of this paper.

References

- [1] Mnasri, T., Ben Younès, R., Mazioud, A. and Durastanti, J.F. (2010) FVM-BEM Method Based on the Green's Function Theory for the Heat Transfer Problem in Buried Co-Axial Exchanger. *Comptes Rendus Mécanique*, **338**, 220-229. <https://doi.org/10.1016/j.crme.2010.04.004>
- [2] Desmons, J.Y. and Ben Younis, R. (1997) Prévision à long terme de la réponse d'un stockage de chaleur sensible dans le sol. *International Journal of Heat and Mass Transfer*, **40**, 3119-3134. [https://doi.org/10.1016/S0017-9310\(96\)00334-1](https://doi.org/10.1016/S0017-9310(96)00334-1)
- [3] Subramanian, S.R. (2012) The Graetz Problem. [https://web2.clarkson.edu/projects/subramanian/ch490/notes/Graetz Problem.pdf](https://web2.clarkson.edu/projects/subramanian/ch490/notes/Graetz%20Problem.pdf)
- [4] Sieder, E.N. and Tate, G.E. (1936) Heat Transfer and Pressure Drop of Liquids in Tubes. *Industrial & Engineering Chemistry Research*, **28**, 1429-1435. <https://doi.org/10.1021/ie50324a027>
- [5] Hausen, H. (1943) Darstellung des Wärmeüberganges in Rohren durch verallgemeinerte Potenzbeziehungen, VDI. *Verfahr*, **4**, 91-98.
- [6] Gnielinski, V. (1984) Forced Convection in Ducts, Heat Exchanger Design Hand Book. Hemisphere Publishing Corporation, London.
- [7] Kim, W.K., Martin, H. and Gnielinski, V. (1993) Pressure Drop and Heat Transfer in Shell and Tube Heat Exchangers without Baffles. Part I. The Graetz-Nusselt Problem in Acylindrical Shell Containing a Bundle of Seven Tubes. *Chemical Engineering and Processing*, **32**, 99-110. [https://doi.org/10.1016/0255-2701\(93\)85020-G](https://doi.org/10.1016/0255-2701(93)85020-G)
- [8] Mnasri, T., Ben Younès, R., Raddaoui, M. and Elouragini, S. (2007) Simulation of

Convective Heat-Transfer Coefficient in a Buried Exchanger. *American Journal of Applied Sciences*, **5**, 927-933. <https://doi.org/10.3844/ajassp.2008.927.933>

- [9] Naili, N., Hazami, M., Attar, I. and Farhat, A. (2013) In-Field Performance Analysis of Ground Source Cooling System with Horizontal Ground Heat Exchanger in Tunisia. *Energy*, **61**, 319-333. <https://doi.org/10.1016/j.energy.2013.08.054>
- [10] Boughanmi, H., Lazaar, M. and Guizani, A. (2018) A Performance of a Heat Pump System Connected a New Conic Helicoidal Geothermal Heat Exchanger for a Greenhouse Heating in the North of Tunisia. *Solar Energy*, **171**, 343-353. <https://doi.org/10.1016/j.solener.2018.06.054>
- [11] Padet, J. (2010) Principe des Transferts Convectifs. Seconde Edition, Société Française de Thermique, France. <https://www.sft.asso.fr/>
- [12] Dhahri, I. and Ammar, L. (2017) Distribution of the Temperature in the Coaxial Tube Heat Exchanger with Spherical End. *Case Studies in Thermal Engineering*, **10**, 621-627. <https://doi.org/10.1016/j.csite.2017.11.003>

Nomenclature

a_{so}	Diffusivity of the ground (m^2/s)	T_e	Inlet temperature of the fluid in the inner tube (K)
a_f	Diffusivity of the fluid (m^2/s)	T_m	Mean temperature of the fluid in annular space at z and (K)
D_H	Hydraulic diameter, $D_H = 2(R_i - r_{ex})$. (m)	T_w	Temperature of the exchanger wall at z and t (K)
G	Green's function	T_0	Initial temperature field in the soil $t = 0$ (K)
h	Local heat transfer coefficient at the wall (Wm^{-2}/K)	u	Radial velocity (m/s)
k_f	Thermal conductivity of the fluid. (Wm^{-1}/K)	v	Orthoradial velocity (m/s)
k_s	Thermal conductivity of the ground (Wm^{-1}/K)	w	Axial velocity in annular space (m/s)
L	Length of the exchanger. (m)	u_0	Average velocity of fluid in the annularspace (m/s)
\vec{r}	Vector-position in the space	z	Axial coordinate (m)
\vec{r}'	Vector-position in the space where the temperature is evaluated	<i>Greek</i>	Symbols
Re	Reynolds number, $Re = W_0 D_H \rho / \mu$, dimensionless	δ	Time step (s)
r_{ex}	Radius of the central tube. (m)	Φ	Heat flux density (W/m^2)
R_i	Radius of the exchanger (m)	ν	f cinematic viscosity of the fluid (m^2/s)
t	Time (s)	ρ_f	Fluid density (kg/m^3)